Soluble (pro)renin receptor via β-catenin enhances urine concentration capability as a target of liver X receptor

Xiaohan Lu[a,b,c,1], Fei Wang[c,a,b,1], Chuanming Xu[c], Sunny Soodvilai[a,b], Kexin Peng[a,b,c], Jiahui Su[c], Long Zhao[a,b], Kevin T. Yang[a,b], Yumei Feng[d,e], Shu-Feng Zhou[f], Jan-Åke Gustafsson[g,2], and Tianxin Yang[a,b,c,2]

[a]Department of Internal Medicine, University of Utah, Salt Lake City, UT 84112; [b]Veterans Affairs Medical Center, Salt Lake City, UT 84108; [c]Institute of Hypertension, Zhongshan School of Medicine, Sun Yat-sen University, Guangzhou, 510080, People's Republic of China; [d]Department of Pharmacology, University of Nevada School of Medicine, Reno, NV 89557; [e]Department of Physiology and Cell Biology, University of Nevada School of Medicine, Reno, NV 89557; [f]Department of Pharmaceutical Sciences, College of Pharmacy, University of South Florida, Tampa, FL 33620; and [g]Department of Biology and Biochemistry, University of Houston, Houston, TX 77004

Contributed by Jan-Åke Gustafsson, February 12, 2016 (sent for review February 1, 2016; reviewed by Guanping Chen and Jia L. Zhuo)

The extracellular domain of the (pro)renin receptor (PRR) is cleaved to produce a soluble (pro)renin receptor (sPRR) that is detected in biological fluid and elevated under certain pathological conditions. The present study was performed to define the antidiuretic action of sPRR and its potential interaction with liver X receptors (LXRs), which are known regulators of urine-concentrating capability. Water deprivation consistently elevated urinary sPRR excretion in mice and humans. A template-based algorithm for protein–protein interaction predicted the interaction between sPRR and frizzled-8 (FZD8), which subsequently was confirmed by coimmunoprecipitation. A recombinant histidine-tagged sPRR (sPRR-His) in the nanomolar range induced a remarkable increase in the abundance of renal aquaporin 2 (AQP2) protein in primary rat inner medullary collecting duct cells. The AQP2 up-regulation relied on sequential activation of FZD8-dependent β-catenin signaling and cAMP–PKA pathways. Inhibition of FZD8 or tankyrase in rats induced polyuria, polydipsia, and hyperosmotic urine. Administration of sPRR-His alleviated the symptoms of diabetes insipidus induced in mice by vasopressin 2 receptor antagonism. Administration of the LXR agonist TO901317 to C57/BL6 mice induced polyuria and suppressed renal AQP2 expression associated with reduced renal PRR expression and urinary sPRR excretion. Administration of sPRR-His reversed most of the effects of TO901317. In cultured collecting duct cells, TO901317 suppressed PRR protein expression, sPRR release, and PRR transcriptional activity. Overall we demonstrate, for the first time to our knowledge, that sPRR exerts antidiuretic action via FZD8-dependent stimulation of AQP2 expression and that inhibition of this pathway contributes to the pathogenesis of diabetes insipidus induced by LXR agonism.

soluble (pro)renin receptor | liver X receptor | aquaporin-2 | frizzled-8 | β-catenin

Full-length (Pro)renin receptor (PRR), a 350-amino acid transmembrane receptor for prorenin and renin, is subjected to protease-mediated cleavage to produce a 28-kDa protein of the N-terminal extracellular domain, the soluble (pro)renin receptor (sPRR), and the 8.9-kDa C-terminal intracellular domain called "M8.9" (1, 2). Before the cloning of full-length PRR in mesangial cells as an integral 39-kDa membrane protein (3), M8.9 was identified as a truncated protein associated with the vacuolar H^+-ATPase (V-ATPase) from bovine chromatin granules (4). The cleavage occurs in Golgi apparatus through furin (5) or ADMA19 (6). An sPRR ELISA kit has been developed to detect sPRR in plasma and urine samples (7). With this assay, increased serum sPRR levels have been demonstrated in patients with heart failure (8), kidney disease (9, 10), hypertension (11), and preeclampsia (2). Moreover, serum sPRR is positively associated with serum creatinine, blood urea nitrogen, and urine protein and is inversely associated with the estimated glomerular filtration rate in patients with chronic kidney disease caused by hypertension and type 2 diabetes (9). However, serum sPRR was not correlated with serum renin, prorenin, or aldosterone in healthy subjects or in patients with diabetes and hypertension (12). To our knowledge no prior studies have reported a biological function of sPRR in any condition.

Within the kidney, PRR is expressed abundantly in the distal nephron, particularly in intercalated cells of the collecting duct (CD) (13, 14). A functional role of PRR in regulating renal aquaporin 2 (AQP2) expression and urine-concentrating capability has been revealed by analysis of mice with conditional deletion of PRR in the nephron (15) and the CD (14). However, whether the antidiuretic action of CD PRR is conferred by sPRR remains elusive.

Liver X receptors (LXRs) are activated by oxidized cholesterol derivatives and belong to a family of nuclear receptors that form heterodimers with the retinoid X receptor to regulate transcription of target genes governing cholesterol, fatty acid, and glucose metabolism (16, 17) (18). LXRs consist of two isoforms, LXRα, which is abundantly expressed in liver, small intestine, kidney, macrophages, and adipose tissue, and LXRβ, which is expressed more ubiquitously (19). LXRs have an established role in reverse cholesterol transport which leads to cholesterol efflux from peripheral tissues to the liver (20). Interestingly, emerging

Significance

The soluble (pro)renin receptor (sPRR) is produced by protease-mediated cleavage of PRR and is elevated under certain pathological conditions. To our knowledge, no prior studies have reported the biological function of sPRR in general or the antidiuretic function of the soluble protein in particular. Here we describe a previously unreported role of sPRR in the enhancement of renal aquaporin 2 (AQP2) expression and urine-concentrating capability. We further show that sPRR acts via frizzled class receptor 8-depdendent β-catenin signaling to increase AQP2 expression in the collecting duct cells. These findings offer an unreported insight into the physiological role of sPRR in regulating fluid homeostasis. In addition, we found that liver X receptor activation by TO901317 resulted in diabetes insipidus because of the inhibition of renal PRR expression.

Author contributions: S.-F.Z., J.-Å.G., and T.Y. designed research; X.L., F.W., C.X., S.S., K.P., J.S., L.Z., and K.T.Y. performed research; Y.F. contributed new reagents/analytic tools; and J.-Å.G. and T.Y. wrote the paper.

Reviewers: G.C., Emory University School of Medicine; and J.L.Z., University of Mississippi.

The authors declare no conflict of interest.

[1]X.L. and F.W. contributed equally to this work.

[2]To whom correspondence may be addressed. Email: jgustafsson@uh.edu or Tianxin.Yang@hsc.utah.edu.

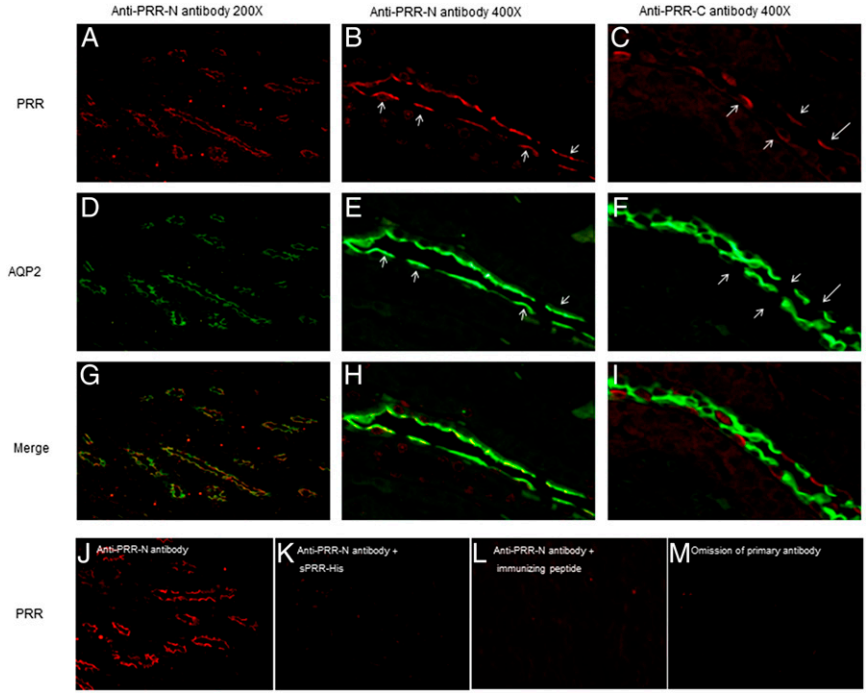

Fig. 1. Distinct labeling with antibodies against different domains of PRR. (*A*–*C*) Immunostaining on consecutive rat kidney sections using anti–PRR-N antibody (magnification: 200× in *A*; 400× in *B*) recognizing the N-terminal domain of PRR (e.g., the sPRR sequence) and the anti–PRR-C antibody recognizing the C-terminal domain of PRR (*C*; magnification: 400×). (*D*–*F*) The PRR antibodies were coincubated with anti-AQP2 antibody. (*G*–*I*) Merged images. Arrows in *B* and *E* denote principal cells; arrows in *C* and *F* denote intercalated cells. The labeling with anti–PRR-N antibody was localized mostly to the apical membrane of principal cells, contrasting with the labeling with anti–PRR-C antibody in the intercalated cells. (*J*–*M*) To validate the specificity of the labeling, immunostaining was performed with anti–PRR-N antibody preincubated with an expressed sPRR (*J*), sPRR-His (*K*), or its immunizing peptides (*L*) or without the primary antibody (*M*). The images shown are representative of three to six animals per group.

evidence suggests a potential role of LXRs in the regulation of the renin-angiotensin system (RAS) and renal transporters such as Na-Pi transporters (21), OAT1 (22), and epithelial Na^+ channel (ENaC) (23). In the present study we attempted to define a biological function and signaling of sPRR in the regulation of fluid homeostasis and to test PRR/sPRR further as a target of LXRs in the kidney.

Results

Initial Evidence for a Biological Function of sPRR. A clue indicating a potential biological function of sPRR came from immunostaining of rat kidneys using antibodies against different domains of PRR. We examined the cellular localization of renal PRR in rats using two different antibodies: the antibody raised against the C-terminal domain of PRR (termed "anti–PRR-C antibody"; Abcam) and another antibody against the N-terminal domain in the sPRR sequence (termed "anti–PRR-N antibody") (24). After the cleavage, sPRR is recognized by anti–PPR-N but not by anti–PRR-C. Anti–PRR-C antibody labeled $AQP2^-$ CD cells, e.g., the intercalated cells (Fig. 1*C*) (13, 25). Unexpectedly, the labeling with anti–PRR-N was found predominantly on the apical membrane of CD principal cells (Fig. 1 *A* and *B*), overlapping with AQP2 (Fig. 1 *D* and *E*), confirming the localization in principal cells but not in intercalated cells. The images from colabeling with anti-PRR antibody and anti-AQP2 antibody were merged (Fig. 1 *G*–*I*). We performed a competition assay to validate the specificity of anti–PRR-N antibody. The signal from this antibody disappeared after preincubation with a recombinant sPRR protein, sPRR-His (Fig. 1 *J* and *K*) or with the immunizing peptide (Fig. 1*L*) or with the omission of primary antibody (Fig. 1*M*).

These immunostaining results raised the intriguing possibility that sPRR derived from intercalated cells or other tubules may act on an as yet unknown membrane receptor in principal cells to regulate tubular transport function. To test this possibility, a recombinant rat sPRR was generated using a mammalian cell-expressing system. This protein contained sPRR with a secretion signal in the N terminus and an eight-histidine tag in the C terminus (termed "sPRR-His") and appeared as a single 29.6-kDa band on 12% SDS/PAGE gel (Fig. 2*A*). Primary cultures of rat inner medullary collecting duct (IMCD) cells in Transwells exposed to 10 nM sPRR-His for 24 h exhibited a remarkable increase in AQP2 expression at both mRNA and protein levels (Fig. 2 *B* and *C*). In a separate experiment, murine immortalized cortical collecting duct (mpkCCD) cells were transiently transfected by a luciferase reporter construct, pGL3-AQP2. The transfected cells were treated for 24 h with 10 nM sPRR-His or vehicle. The sPRR-His treatment induced a 5.5-fold increase in luciferase activity (Fig. 2*D*). The in vitro findings confirmed a direct stimulatory effect of sPRR-His on AQP2 expression.

sPRR Activation of the Wnt–β-Catenin Pathway in the CD. Search tool for the retrieval of interacting gene and proteins (STRING) is a template-based algorithm for protein–protein structure prediction. We used STRING to identify proteins that interact with sPRR. Among 10 candidate proteins, three are related to Wnt–β-catenin pathway: frizzled-8 (FZD8), low-density lipoprotein receptor-related protein 6 (LRP6), and Wnt-3a (Fig. 2*E*). Because FZD8 is a receptor component in the Wnt–β-catenin pathway, subsequent studies were focused on interaction between FZD8 and sPRR. Coimmunoprecipitation experiments using membrane fraction proteins prepared from the rat inner medulla demonstrated that sPRR binds to FZD8 (Fig. 3*A*). Immunostaining showed that at low magnification (Fig. 3*B*), FZD8 labeling was found predominantly in the outer and inner medulla with sporadic labeling in the cortex. Colabeling with AQP2 (the marker of CD principal cells) and labeling of

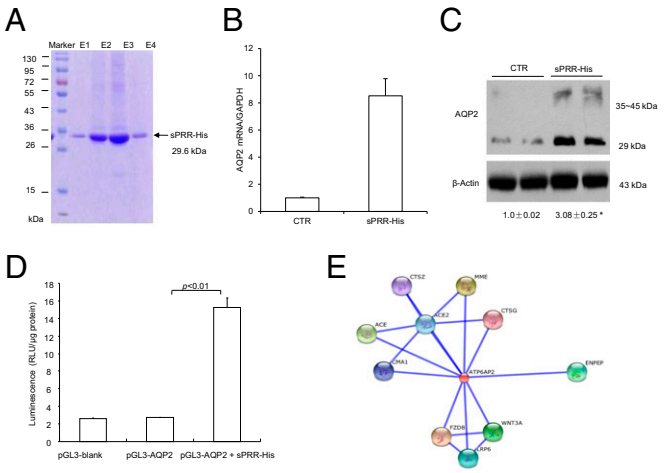

Fig. 2. Characterization of sPRR function. A recombinant PRR, sPRR-His, was expressed in a mammalian cell-expressing system as a fusion protein that contained sPRR, a histidine tag in the C terminus, and a secretion signal peptide in the N terminus. (*A*) sPRR-His was purified from the medium as a single 29.6-kDa band in 12% SDS/PAGE gel. E1–4 are sequential fractions from the elution. (*B* and *C*) Primary rat IMCD cells grown in Transwells were exposed to 10 nM sPRR-His for 24 h, and AQP2 expression was analyzed by quantitative RT-PCR and immunoblotting ($n = 5$ per group). (*D*) In a separate experiment, the cultured CD cells were transfected with an AQP2-luciferase construct, were allowed to grow to confluence, and then were treated with vehicle or 10 nM sPRR-His for 24 h, and luciferase activity was assayed ($n = 5$ per group). (*E*) STRING is a template-based algorithm for predicting protein–protein structure. We used STRING to identify proteins that interact with sPRR. This analysis revealed 10 hits: CTSG (cathepsin G), ACE2 (angiotensin 1-converting enzyme 2), CMA1 (chymase 1), MME (membrane metallo-endopeptidase), ACE (angiotensin 1 converting enzyme 1), CTSZ (cathepsin Z), ENPEP (glutamyl aminopeptidase), FZD8 (frizzled family receptor 8), WNT3A (wingless-type MMTV integration 3A), and LRP6 (low density lipoprotein receptor-related protein 6). CTR, control.

consecutive sections for the electroneutral sodium, potassium and chloride cotransporters (NKCC2), a marker of thick ascending limb cells (Fig. 3*C*), confirmed FZD8 staining in the thick ascending limb and the CD. In the CD, FZD8 staining was detected in both principal and intercalated cells. The comparison between FZD8 and PRR labeling was made in the inner medulla where the two signals were roughly colocalized to the CD. In principal cells, both FZD8 and PRR were detected on the apical membrane although FZD8 labeling was relatively diffuse (Fig. 3*D*).

The functional role of FZD8 in mediating sPRR signaling in primary rat IMCD cells was assessed by using FZD8 siRNA and an FZD8 inhibitor, OMP-54F03 (OMP). The efficacy of FZD8 siRNA was validated by immunoblotting analysis of FZD8 protein expression (Fig. 4*A*). Exposure of rat IMCD cells to 10 nM sPRR-His for 24 h induced the activity of Wnt-responsive luciferase activity as assessed by using the Cignal TCF/LEF Reporter Assay kit (Qiagen), which was blunted by FZD siRNA (Fig. 4*B*). Consistent with this result, the sPRR-His treatment remarkably induced AQP2 protein expression, which was blunted by both FZD8 siRNA (Fig. 4*C*) and OMP (Fig. 4*D*) as well as by a tankyrase inhibitor XAV939 (XAV) (Fig. 4*E*) (26). Tankyrase belongs to the poly (ADP-ribose) polymerase family responsible for the transfer of ADP ribose from NAD^+ to acceptor proteins (27) and also for the activation of the Wnt–β-catenin pathway through the stabilization of the axin–β-catenin complex (26). Our results suggest that sPRR signals through FZD8 to activate the Wnt/β–catenin pathway, leading to increased AQP2 expression.

Arginine vasopressin (AVP) is known to induce AQP2 trafficking to the apical membrane acutely (within minutes) by increasing phosphorylation of AQP2 and chronically (within hours) by stimulating AQP2 transcription, both through the cAMP–PKA pathway (28, 29). We found that the rapid rise of cAMP and the redistribution of AQP2 from the cytosol to the membrane in response to a 30-min exposure to AVP was unaffected by XAV treatment (Fig. 5 *A*–*C*); the trafficking event was evaluated by examining the abundance of AQP2 protein in the fractionated cell samples. Immunoblotting detected AQP2 protein as multiple bands of 35–45 kDa and 29 kDa, reflecting the glycosylated and nonglycosylated forms, respectively. In contrast, at 24 h the increases in the cAMP level (Fig. 5*D*) and total protein abundance (Fig. 5*E*) and mRNA expression (Fig. 5*F*) of AQP2 were all effectively attenuated by XAV treatment. These results suggest that the Wnt–β-catenin pathway may specifically target AQP2 gene transcription but not AQP2 trafficking via selective coupling with the late but not early cAMP production after AVP treatment.

The in Vivo Role of β-Catenin Signaling in Rats During Antidiuresis. To probe the in vivo role of β-catenin signaling in fluid homeostasis, we administered OMP and XAV to Sprague–Dawley (SD) rats under basal conditions and during 48-h water deprivation (WD) and evaluated their impact on water balance. Under basal conditions, the administration of OMP and XAV over 48 h similarly induced polyuria, polydipsia, and hypoosmotic urine (Fig. 6 *A*–*C*). During 48-h WD, these treatments consistently increased urine volume and decreased urine osmolality, and these effects were accompanied by exaggerated weight loss (Fig. 6 *D*–*F*) and greater increases in plasma osmolality and hematocrit (Hct) (Fig. 6 *G* and *H*). Immunoblotting showed that the abundance of β-catenin protein was increased in the nuclear fraction from both cortex and inner medulla following WD, indicating the activation of β-catenin signaling (Fig. 7 *A* and *B*). AQP2 protein abundance in both renal cortex and inner medulla was increased remarkably following WD; this increase was attenuated significantly by both OMP and XAV (Fig. 7 *C*–*F*).

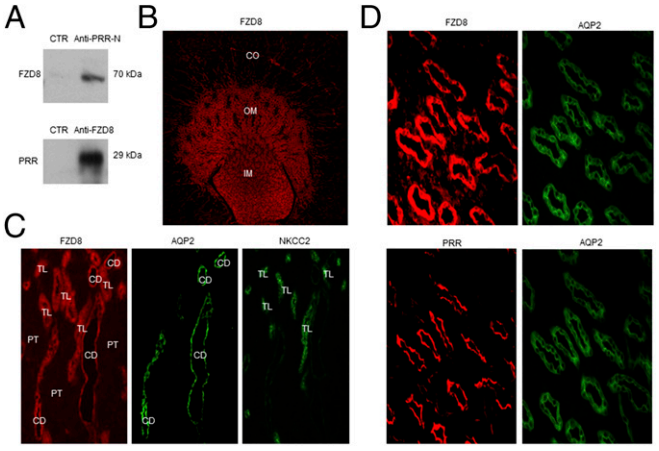

Fig. 3. Renal FZD8 expression and its interaction with sPRR. (*A*) Coimmunoprecipitation analysis of the interaction between sPRR and FZD8. The membrane fraction of rat renal medulla was immunoprecipitated with anti–PRR-N antibody and probed with anti-FZD8 antibody or vice versa. (*B*) Immunolabeling of FZD8 in rat kidney at low magnification. (*C*) Immunolabeling of FDZ8, AQP2, and NKCC2 in the outer medulla at high magnification. Colabeling for AQP2 was performed on the same section, and labeling for NKCC2 was performed on consecutive sections. CD, collecting duct; PT, proximal tubule; TL, thick ascending limb. (*D*) Immunolabeling of FDZ8 and PRR in the rat inner medulla. The consecutive sections were stained with anti-FZD8 antibody and anti–PRR-N antibody. The same section was colabeled with anti-AQP2 antibody. The images shown are representative of three to six animals per group.

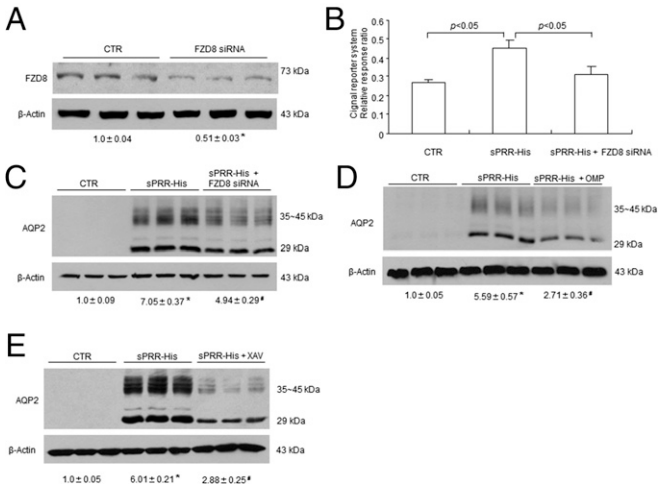

Fig. 4. Analysis of the in vitro role of the Wnt/β–catenin pathway in the regulation of AQP2 expression in response to sPRR-His treatment. (*A*) Validation of FZD8 knockdown by siRNA ($n = 3$ per group). Primary rat IMCD cells were transfected with or without FZD8 siRNA. FZD8 protein expression was evaluated by immunoblotting. (*B*) Effect of sPRR-His on Wnt-response luciferase activity in the presence or absence of FZD8 siRNA ($n = 12$ per group). The IMCD cells were transfected with or without FZD8 siRNA, followed by sPRR-His treatment at 10 nM for 24 h. The Cignal reporter system was used to evaluate the activity of the Wnt/β–catenin pathway, and the data are presented as relative response ratio. (*C–E*) Rat IMCD cells were transfected with FZD8 siRNA, pretreated with OMP or XAV-939 for 1 h, and treated with 10 nM sPRR for 24 h. AQP2 protein expression was determined by immunoblotting analysis. Densitometric values are shown underneath the blots. (*C*) Effect of FZD8 knockdown on sPRR-Induced AQP2 protein expression ($n = 6$ per group). (*D*) Effect of OMP on sPRR-His-induced AQP2 protein expression ($n = 6$ per group). (*E*) Effect of XAV on sPRR-His-induced AQP2 expression ($n = 6$ per group). Data are shown as mean ± SE; $^*P < 0.05$ vs. control; $^{\#}P < 0.05$ vs. sPRR-His.

Therapeutic Potential of sPRR-His for Treatment of Nephrogenic Diabetes Insipidus. Nephrogenic diabetes insipidus (NDI) is commonly caused by mutations of the vasopressin 2 receptor (V2R) gene; a specific therapy for this disease is lacking (30, 31). We explored the therapeutic potential of sPRR-His in a mouse model of NDI induced with a V2R antagonist, OPC. sPRR-His was chronically infused via a catheter placed in the jugular vein driven by an osmotic minipump. After 7 d of sPRR-His infusion, OPC was given via gavage at 30 $mg \cdot kg^{-1} \cdot d^{-1}$ for 3 d. Administration of the V2R antagonist resulted in symptoms of NDI, including polydipsia, polyuria, and hypoosmotic urine, all of which were attenuated by sPRR-His treatment (Fig. 8 *A–C*). This result supports the therapeutic potential of sPRR for management of the symptoms of NDI. In the OPC-treated mice, urinary sPRR excretion was suppressed significantly (Fig. 8*D*), providing a rationale for the use of exogenous sPRR to treat NDI. This result also suggests that the production of renal sPRR may be under the direct control of the AVP–V2R pathway. In support of this notion, we have shown that exposure of the CD cells to AVP stimulates the release of sPRR (14). Fig. 8*E* provides a schematic illustration of the mechanism of action of sPRR in the CD principal cells. Our data suggest that sPRR binds FDZ8, leading to the activation of β-catenin that promotes chronic cAMP accumulation, ultimately enhancing AQP2 transcription.

Induction of Diabetes Insipidus and Suppression of Renal PRR by LXR Agonism. Besides their well-recognized role in regulating lipid and glucose metabolism, LXRs are potential regulators of the RAS (32) and fluid balance (33). We tested the hypothesis that LXRs may affect renal PRR expression and local RAS and hence fluid homeostasis. In the initial experiment, we examined the effects of the LXR agonist TO901317 on fluid homeostasis and on renal PRR and urinary renin levels in mice. A 7-d treatment with TO901317 in C57BL6 mice reduced body weight (32.36 ± 0.63 vs. 28.61 ± 0.36 g, $P < 0.05$) and food intake (4.08 ± 0.19 vs. 3.54 ± 0.15 g, $P < 0.05$), as previously reported (34), although to a lesser extent. This treatment led to severe polyuria (Fig. 9*A*) and hypoosmotic urine (Fig. 9*B*), indicating a urine-concentrating defect. The expression of renal PRR protein and the excretion of urinary sPRR were examined by immunoblotting and ELISA, respectively. Both renal PRR expression (Fig. 9 *C* and *D*) and urinary sPRR excretion (Fig. 9*E*) were suppressed consistently by TO901317. This experiment suggested that the suppressed renal PRR level may be responsible for TO901317-induced diabetes insipidus (DI).

We performed cell-culture experiments to examine the direct effect of TO901317 on PRR expression. mpkCCD cells were exposed to TO901317 or vehicle for 24 h, and PRR protein expression was determined by immunoblotting. TO901317 treatment reduced PRR protein expression by 85% (Fig. 9 *F* and *G*) and medium sPRR by 60% (Fig. 9*H*). In a separate experiment, mpkCCD cells were transiently transfected by a pGL3-PRR construct. The transfected cells were treated with TO901317 or vehicle for 24 h. TO901317 treatment suppressed luciferase activity by 76% (Fig. 9*I*). The in vitro findings confirmed that TO901317 has a direct inhibitory effect on PRR expression.

sPRR-His Attenuates TO901317-Induced DI in Mice. In the subsequent experiment, we performed more detailed analysis of TO901317-induced DI and further examined the causal role of suppressed renal PRR in this phenomenon. This experiment comprised three groups: control, TO901317-treated, and TO901317 + sPRR-His–treated mice. TO901317-treated mice displayed polyuria, polydipsia, decreased water balance, hypoosmotic urine, and plasma volume contraction (as reflected by the rise in Hct), confirming the urine-concentrating defect (Fig. 10). All these parameters were improved significantly in mice treated withTO901317 + sPRR-His

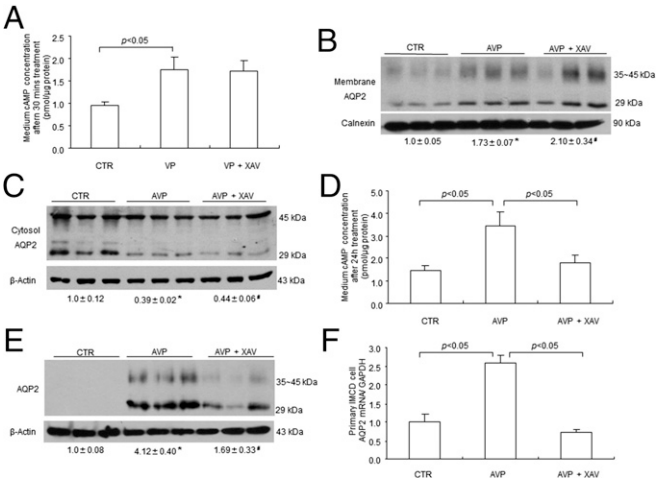

Fig. 5. The distinct role of the Wnt/ β–catenin pathway in the acute and chronic responses to AVP in primary rat IMCD cells. The IMCD cells were pretreated for 1 h with XAV and were treated for 30 min or 24 h with 10 nM AVP. (*A*) At 30 min of AVP treatment, the medium was assayed for cAMP using ELISA ($n = 6$ per group). (*B* and *C*) Membrane fraction ($n = 6$ per group) (*B*) and cytosolic fraction ($n = 6$ per group) (*C*) were subjected to immunoblotting analysis of AQP2. (*D–F*) At 24 h, medium cAMP was determined ($n = 6$ per group) (*D*), whole-cell lysates were subjected to immunoblotting analysis of AQP2 ($n = 6$ per group) (*E*), and total RNA was subjected to quantitative RT-PCR analysis of AQP2 mRNA ($n = 4$ per group) (*F*). Data are shown as mean ± SE; $^*P < 0.05$ vs. control; $^{\#}P < 0.05$ vs. AVP alone.

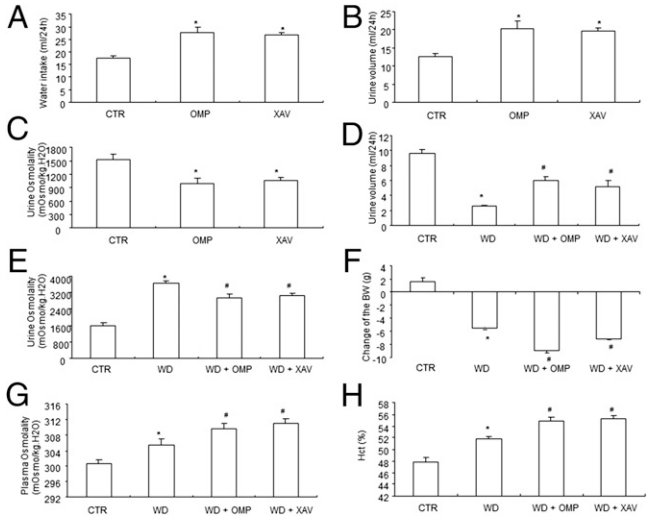

Fig. 6. The role of the Wnt/β–catenin pathway in urine-concentrating capability in rats. SD Rats were administered vehicle, OMP, or XAV and were placed in metabolic cages for assessment of the state of water metabolism at basal condition (*A*–*C*) or after 24-h WD (*D*–*H*) ($n = 5$ rats per group). At basal the condition, water intake (*A*), urine volume (*B*), and urine osmolality (*C*) were determined. (*D*–*F*) During 24-h WD, urine volume (*D*), urine osmolality (*E*), and body-weight (BW) changes (*F*) were monitored. (*G* and *H*) At the end of the experiment plasma osmolality (*G*) and Hct (*H*) were measured. $^{*}P <$ 0.05 vs. control; $^{\#}P < 0.05$ vs. WD alone.

(Fig. 10). Of note, water balance was determined by subtracting urine volume from water intake. AQP2, a major water channel on the apical membrane of the CD, plays a key role in determining urine-concentrating capability. Immunoblotting demonstrated that TO901317 significantly reduced renal AQP2 expression, which was partially restored by sPRR-His (Fig. 11 *A* and *B*). We suspected that sPRR-His may affect the intrarenal RAS, and this effect can be reflected by urinary renin activity (35). Urinary renin activity, as assessed by measuring the generation of angiotensin I (AngI), was suppressed by TO901317, and the suppression was completely reversed by sPRR-His (Fig. 11*C*). We also performed ELISA to determine the prorenin/renin concentration in the urine. Although urinary prorenin/renin excretion was suppressed by TO901317, it was unaffected by sPRR-His (Fig. 11*D*). This result is compatible with the concept that sPRR regulates renin primarily at its activity level (3). Fig. 11*E* provides a schematic illustration of the mechanism by which TO901317 induces DI. Upon binding to TO901317, LXRs function as a transcriptional repressor to inactivate PRR transcription. The reduced PRR/sPRR levels down-regulate AQP2 expression, leading to DI.

Discussion

sPRR is generated by protease-mediated cleavage in the Golgi apparatus and is released to plasma or urine. Serum sPRR levels are elevated in various pathological states. To our knowledge, no prior studies have reported a biological function of sPRR. We recently used pharmacological and conditional gene-knockout approaches to demonstrate that CD PRR has an essential role in determining renal AQP2 expression and urine-concentrating capability (14). In the present study, we discovered that sPRR acts via FZD8-dependent activation of β-catenin signaling that leads to increased AQP2 expression and thus enhanced urine-concentrating capability. In addition, we found that LXR agonism with TO901317 induced DI by inhibiting the renal PRR and the intrarenal RAS.

Probably the most striking finding of this study was the remarkable stimulatory effect of sPRR-His on AQP2 expression in cultured rat IMCD cells grown in Transwells. In this experiment, sPRR-His was used at 10 nM, which is likely a physiological concentration. Moreover, we vigorously examined the signaling mechanism of sPRR-His up-regulation of AQP2, revealing the involvement of FZD8-dependent β-catenin signaling. A clue suggesting potential interaction between sPRR and FZD8 was obtained by a template-based algorithm for predicting protein–protein structure. The physical interaction of the two proteins in the membrane fraction of the rat inner medulla was confirmed by coimmunoprecipitation. The interaction also was demonstrated at a functional level, because inhibition of FZD8 by siRNA and pharmacological approaches effectively attenuated the stimulatory effect of sPRR-His on AQP2 in cultured CD cells. The functional role of FZD8 in regulating renal AQP2 expression and urine-concentrating capability was confirmed in vivo by using a FZD8 inhibitor, OMP. The antidiuretic function of FZD8 was supported by the similar effect of a general Wnt/β-catenin inhibitor, XAV. Immunostaining demonstrated that FZD8 is localized to the CD and thick ascending limb, as is consistent with the nephron-distribution pattern of PRR. Within the CD, FZD8 labeling was found in both principal and intercalated cells, a pattern not exactly same as sPRR labeling. We suspect that FZD8 may serve a function beyond its association with sPRR. These results agree with a previous report that β-catenin signaling mediated AVP-induced AQP2 expression in mpkCCDc14 cells (36). It is evident that β-catenin signaling is actively involved in the physiological regulation of fluid homeostasis through coupling with sPRR.

A large body of evidence has demonstrated that PRR serves as a component of the Wnt receptor complex to regulate embryogenesis in low vertebrates in which the RAS does not exist (37, 38). It is evident that PRR acts in a renin-independent manner in low vertebrates (1, 37, 39-41). PRR appears to be similarly involved in the regulation of embryogenesis in mammals, as evidenced by the lethal phenotype in mice with systemic or tissue-specific deletion of PRR (1, 4). A large number of studies have challenged the physiological function of PRR and its

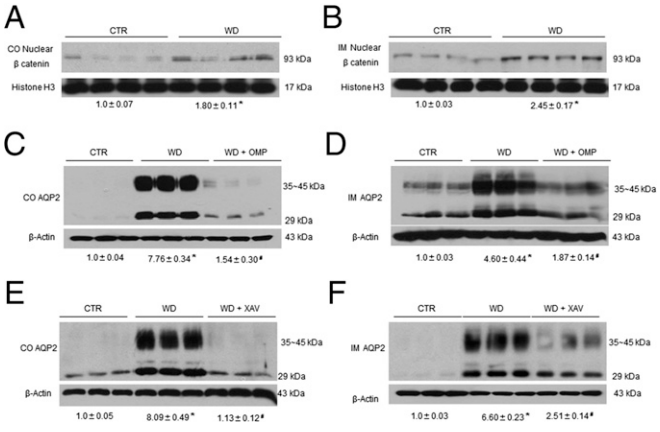

Fig. 7. The in vivo role of the Wnt/β–catenin pathway in the regulation of renal AQP2 expression during antidiuresis in rats. (*A* and *B*) To assess renal β-catenin activation by WD, the nuclear fraction of renal cortex ($n = 4$ rats per group) (*A*) and the inner medulla ($n = 4$ rats per group) (*B*) from control and dehydrated rats were subjected to immunoblotting analysis of β-catenin. (*C*–*F*) Immunoblotting analysis of AQP2 expression was performed on the renal cortex and the inner medulla of rats treated with vehicle or WD with (*C*) or without (*D*) OMP or with (*E*) or without (*F*) XAV ($n = 5$ rats per group). Data are shown as mean ± SE; $^{*}P < 0.05$ vs. control; $^{\#}P < 0.05$ vs. WD. CO, cortex; IM, inner medulla.

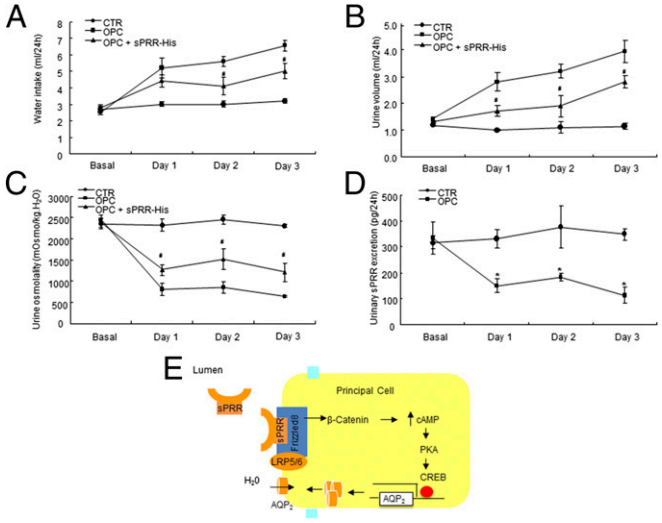

Fig. 8. Antidiuretic action of sPRR-His in a mouse model of NDI. Male C57/BL6 mice were infused for 7 d with sPRR-His via a catheter implanted in the jugular vein and then received oral administration of either vehicle or the V2R antagonist OPC31260 (OPC) for 3 d. Mice were placed in metabolic cages for assessment of daily water intake and urine output. (*A*) Daily water intake (n = 4 mice per group). (*B*) Daily urine output (n = 4 mice per group). (*C*) Urine osmolality (n = 4 mice per group). (*D*) Urinary sPRR excretion (n = 4 mice per group). Data are shown as mean ± SE. In *A*–*C*, $^{\#}P < 0.05$ vs. OPC alone; in *D* $^{*}P < 0.05$ vs. control. (*E*) Schematic illustration of the mechanism of action of sPRR. In the lumen of the distal nephron, sPRR binds FZD8 in a receptor complex on the apical membrane of principal cells, resulting in the activation of β-catenin, which promotes cAMP accumulation, ultimately leading to increased AQP2 transcription and enhanced urine concentration.

relationship with the RAS (1, 37, 39–41). Whether an intrinsic linkage between the RAS and the developmental β-catenin pathway occurs in mammals in settings of development or physiology is unknown. For the first time, to our knowledge, our results link prorenin/sPRR to the β-catenin pathway in the kidney during physiological regulation of fluid homeostasis.

The cAMP–PKA pathway is the principle mediator of AVP-induced AQP2 trafficking and transcription (28, 42, 43). An issue arises as to whether the Wnt–β-catenin pathway interacts with the cAMP–PKA pathway during AVP-induced signaling. We found that inhibition of the Wnt–β-catenin pathway did not affect AQP2 trafficking to the membrane fraction or cAMP production induced by 30-min exposure to AVP. In contrast, this maneuver did block AQP2 expression and cAMP production induced by 24-h AVP treatment. These results suggest that activation of the Wnt–β-catenin pathway may be involved primarily in sustaining the cAMP production during prolonged AVP treatment to increase AQP2 transcription. This mechanism does not appear to be required for the regulation of AQP2 trafficking, which is a rapid response to AVP. There is a wealth of information regarding the role of the cAMP–PKA pathway in this acute response to AVP, but relatively little is known about this pathway in a chronic setting of AVP treatment. To our knowledge, the present study is the first to delineate a unique role for β-catenin signaling in chronic but not acute regulation of the cAMP–PKA–AQP2 axis.

Multiple previous studies, as well as this one, consistently demonstrate that, within the CD, PRR is detected in intercalated cells by using antibody against the C terminus of PRR (anti–PRR-C antibody) (13, 25). A question arises as to how intercalated cell-derived PRR up-regulates AQP2 expression in the principal cells. This regulation may be through a paracrine mechanism, and there is an intriguing possibility that sPRR may serve as a mediator of the communication between the two cell types in the CD. In support of this possibility, an antibody against the epitope in the sPRR, anti–PRR-N antibody, stained only principal cells but not intercalated cells or other non-CD tubules that are known to express PRR. More direct evidence came from cell-culture experiments showing that exposure of rat IMCD cells to sPRR-His in the nanomolar range induced a remarkable increase in AQP2 expression mimicking the effect of prorenin (44). This result strongly suggests that sPRR has a physiological function.

The current therapy for DI is suboptimal. Although supplementation of AVP is effective for central DI (45), no specific therapy is currently available for nephrogenic DI. The present study demonstrates, for the first time to our knowledge, the therapeutic potential of sPRR-His in a mouse model of nephrogenic DI induced by V2R antagonism. Because sPRR acts downstream of V2R, it also should be effective for treatment of central DI.

A large body of evidence has established a link between energy metabolism and fluid balance. A high-energy state, such as obesity, is associated with disturbance of electrolytes and fluid balance and hypertension (46, 47), whereas a low-energy state, such as fasting, induces natriuresis and diuresis (48, 49). Along this line, activation of PPARγ, a key regulator of glucose metabolism and adipogenesis, causes body weight gain and plasma volume expansion (50, 51). In the present study, we discovered that LXR against TO901317 exerted a profound diuretic action in mice as suggested by polyuria, polydipsia, hypoosmotic urine, and contraction of plasma volume. AQP2, a major water channel on the apical membrane of the CD, was remarkably suppressed, likely conferring the diuretic action of TO901317.

In light of sPRR's action as a key regulator of AQP2 expression and urine-concentrating capability, we suspected that PRR/sPRR

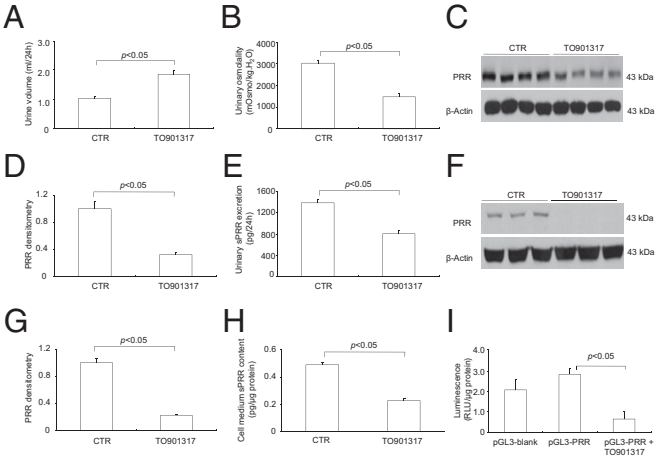

Fig. 9. Initial characterization of diuretic and PRR-inhibitory actions of TO901317 in vivo and in vitro. Male C57/BL7 mice received oral administration of TO901317 with or without i.v. infusion of sPRR-His for 7 d. The mice receiving vehicle treatment served as a control. At the end of experiment, 24-h urine collection was performed, followed by analysis of urinary sPRR excretion by ELISA and renal PRR expression by immunoblotting. (*A*) Urine output (n = 30 mice per group). (*B*) Urinary osmolality (n = 15 mice per group). (*C*) Immunoblotting analysis of renal PRR expression (n = 15 mice per group). (*D*) Densitometric analysis of the immunoblot in *C*. (*E*) ELISA analysis of urinary sPRR (n = 8 mice per group). (*F*–*I*) The effect of TO901317 on PRR expression in cultured CD cells. mpkCCD cells were exposed to vehicle or 10 μM TO901317 for 24 h. The cell lysates were subjected to immunoblotting analysis of PRR protein expression, and the medium was assayed for sPRR concentration by using ELISA and normalized by protein content. In a separate experiment, the cells were transfected with a PRR-luciferase construct, allowed to grown to confluence, and then were treated with vehicle or 10 μM TO901317 for 24 h. (*F*) Immunoblotting analysis of PRR (n = 15 per group). (*G*) Densitometric analysis of the immunoblot in *A*. (*H*) ELISA analysis of medium sPRR (n = 10 per group). (*I*) The luciferase assay (n = 5 per group).

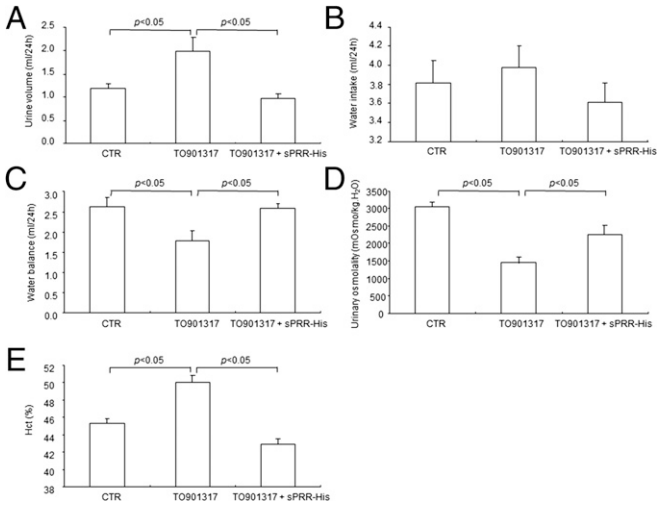

Fig. 10. Effect of sPRR-His on TO901317-induced DI in mice. Male C57/BL6 mice were treated with vehicle or with TO901317 alone or in combination with sPRR-His for 7 d. (*A*) Urine output (n = 8 mice per group). (*B*) Water intake (n = 8 mice per group). (*C*) Water balance (n = 8 mice per group). (*D*) Urinary osmolality (n = 8 mice per group). (*E*) Hct (n = 8 mice per group).

may be a molecular target of LXRs in the kidney. In vivo data showed a significant reduction of renal PRR expression and urinary sPRR excretion in TO901317-treated mice, and the administration of sPRR-His completely rescued TO901317-induced DI. Consistent with this observation, in vitro data demonstrated that TO901317 had a direct inhibitory effect on PRR expression and PPR-luciferase activity in cultured CD cells. These results demonstrate, for the first time to our knowledge, that LXRs may function as a transcriptional repressor of the PRR gene. It is interesting that LXRβ$^{-/-}$ mice display central DI caused by the impairment of AVP production (33). This phenotype suggests an antidiuretic action of LXRβ, which is the opposite of the diuretic action of TO901317. Therefore we speculate that diuretic action of TO901317 may be conferred mainly by LXRα. This possibility needs to be validated in future studies using LXRα-null mice.

It has been shown that acute LXR activation induces a transient increase in renin transcription in the juxtaglomerular cells (32), but its chronic activation remarkably suppresses the expression of renin, AT1R, and angiotensin 1-converting enzyme 1 (ACE) in the heart and kidney following isoproterenol treatment (52). In agreement with the inhibitory effect of LXRs on local RAS, we found that TO901317 treatment remarkably suppressed urinary renin, an index of the intrarenal RAS (35, 53). Although LXRs may function as a negative regulator of renin expression at the juxtaglomerular apparatus in the acute setting, they appear primarily to suppress PRR and the local RAS to elicit a diuretic response.

In summary, the present study reports, for the first time to our knowledge, a biological function of sPRR in regulating fluid homeostasis. sPRR is associated with FZD8 to activate β-catenin, which interacts with the cAMP–PKA pathway to induce AQP2 expression and enhance the urine-concentrating capability. Because intercalated cells are the potential source of sPRR, and principal cells are the site of its action, it seems reasonable to speculate that sPRR mediates the communication between the two cell types in the CD. Last, we discovered the diuretic action of the LXR agonist TO901317, which is conferred by inhibition of the renal PRR/sPRR system.

Methods

Animals. Male 10- to 12-wk-old SD rats and C57BL6 mice were purchased from Charles River Laboratories and the Jackson Laboratory, respectively. All animals were maintained in a temperature-controlled room with a 12:12-h light: dark cycle, with free access to tap water and standard rat chow. Animals were randomized into different experimental groups. Animal protocols were approved by the Animal Care and Use Committees at the University of Utah and the Sun Yat-sen University.

Rat Experiments. Under isoflurane inhalation, rats were s.c. implanted with an osmotic minipump delivering a tankyrase inhibitor, XAV939 (XAV; MedchemExpress) at 5 mg·kg^{-1}·d^{-1} or received a FZD8 inhibitor, OMP54F03 (OMP) (a gift from John Lewicki, OncoMed Pharmaceuticals, Redwood City, CA), at 25 mg/kg via daily i.p. injection. All animals were acclimatized to metabolic cages for 7 d. After collection of baseline data for 2 d, rats were water deprived for 48 h but had free access to chow diets. At the end of the experiment, under isoflurane anesthesia, blood was withdrawn from the vena cava, one kidney was cut into cortex and inner medulla and snap-frozen, and the other kidney was fixed and paraffin embedded.

Plasmid Construction and sPRR Protein Purification. The cDNA of PRR (GenBank accession no. NM_001007091.1; also known as "ATP6AP2") was subcloned into the pMD-18T vector (Takara). sPRR, a solubilized form of sPRR (residues 17–274) lacking the transmembrane domain at the C terminus, was combined with an eight-histidine tag in the C terminus (sPRR-His), was generated by PCR from the PRR expression construct, and then was cloned into pcDNA3.1. sPRR-His was generated by using a mammalian 293 cell system and was purified by binding to IDA-Sephadex G-25 (GE Healthcare) (XBIO, Shanghai, China).

Mouse Experiments. Male C57/BL6 mice received chronic i.v. infusion of vehicle or sPRR-His at 30 μg·kg^{-1}·d^{-1} as described above. After the surgery, the mice were acclimatized to metabolic cages for 7 d and then were randomly divided to receive vehicle or a V2R antagonist, OPC-31260 (Sigma), at 30 mg·kg^{-1}·d^{-1} via gavage for 3 d. Water intake, urine volume, and urine osmolality were recorded daily during the entire experimental period. In another experiment to test the effects of sPRR-His on TO901317-induced DI, male C57/BL6 mice were treated for 7 d with vehicle or with TO901317 alone or in combination with sPRR-His. TO901317 was added to the chow diet at

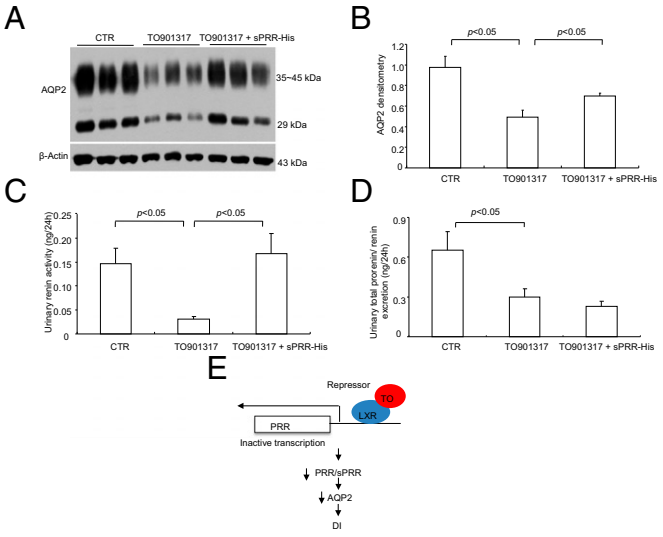

Fig. 11. Effect of sPRR-His on renal AQP2 expression and urinary renin in TO901317-treated mice. Male C57/BL6 mice were treated with vehicle or with TO901317 alone or in combination with sPRR-His for 7 d. AQP2 expression was analyzed by immunoblotting and immunostaining. Urinary renin activity was determined by measuring AngI generation, and urinary prorenin/renin concentration was determined by ELISA. (*A*) Immunoblotting analysis of AQP2 expression (n = 15 mice per group). (*B*) Densitometric analysis of the immunoblots in *A*. (*C*) Urinary renin activity (n = 8 mice per group). (*D*) Urinary prorenin/renin excretion (n = 8 mice per group). (*E*) Schematic illustration of the mechanism by which the LXR agonist TO091317 (TO) suppresses PRR transcription and induces DI. LXRs bound to TO091317 function as a transitional repressor for the PRR gene, leading to a reduced PRR/sPRR level that decreases AQP2 expression, ultimately causing DI.

an estimated level of 50 mg·kg body weight^{-1}·d^{-1}. All mice were placed in metabolic cages, and 24-h water intake and urine output were recorded and collected at the end of the experiments.

Cell-Culture Experiments. For sPRR signaling studies, primary IMCD cells were prepared from 4-wk-old SD rats as previously described (35). The cells were grown in Transwell plates (catalog no. 29442-074; VWR International) with DMEM/F-12 medium containing 10% (vol/vol) FBS, 0.5 μM 8-Br-cAMP, 130 mM NaCl, and 80 mM urea. Upon confluence, the cells were serum deprived for 12 h and pretreated with an inhibitor (10 μM XAV or 10 μM OMP) followed by 24-h treatment with AVP (10 nM) or sPRR-His (10 nM). At the end of the experiments, the medium was collected for biochemical assays.

The effect of TO901337 on PRR expression was tested in mpkCCD cells. These cells were grown to confluence in six-well plates. After 12-h serum deprivation, the cells were treated with vehicle or 10 μM TO901317 for 24 h and then were harvested for analysis of PRR expression and sPRR release. In a separate experiment, mpkCCD cells at ∼50% density were transiently transfected with a construct containing the luciferase gene under the control of the 2,016-bp 5′ flanking region of the PRR gene. Upon confluence, the transfected cells were treated for 24 h with vehicle or 10 μM TO901317 and then were harvested for analysis of luciferase activity.

Enzyme Immunoassay. Urinary or medium sPRR was determined using a commercially sPRR enzyme immunoassay (EIA) kit (catalog no. JP27782; Immuno-Biological Laboratories) according to the manufacturer's instructions.

Immunofluorescence Staining. The tissues were fixed in 10% neutral buffered formalin for 24 h and then were embedded in paraffin. After deparaffinization, thin sections (4 μm) were processed for double-labeling with immunofluorescence. For antigen recovery, the slides were immersed in Tris·HCl EDTA buffer (pH 9.0) at a high temperature (98 °C) for 12 min. The slides were blocked in 1% (wt/vol) BSA for 1 h and then were incubated overnight with primary antibody at 4 °C. After the primary antibody was washed off, sections were incubated for 1 h at room temperature with donkey anti–goat-IgG-FITC (Santa Cruz) or donkey anti-rabbit IgG-TRITC (Life Technologies). Rabbit anti-PRR antibody from Abcam was raised against residues 335–350 in the C terminus (termed "anti–PRR-C antibody"). A second anti-PRR antibody used in the present study raised against residues 218–235 in the N terminus of PRR (termed "anti–PRR-N antibody") was generated in Y.F.'s laboratory (24). Goat anti-AQP2 antibody was purchased from Santa Cruz. Rabbit anti-NKCC2 antibody was purchased from Stress-Marq Biosciences Inc.

Immunoblotting. Renal tissues were lysed and subsequently sonicated. Protein concentrations were determined using Coomassie reagent. Forty micrograms of protein from each sample were denatured in boiling water, separated by SDS/PAGE, and transferred onto nitrocellulose membranes. Blots were blocked 1 h with 5% nonfat dry milk in Tris-buffered saline (TBS), followed by overnight incubation with primary antibody. After washing with TBS, blots were incubated with goat anti-rabbit/mouse HRP-conjugated secondary antibody and visualized using ECL. The blots were quantitated by using Image-Pro Plus (Media Cybernetics). The primary antibodies were goat anti-AQP2 antibody, rabbit anti–PRR-N antibody, and rabbit anti-FZD8 antibody (all from Santa Cruz), rabbit anti-V2R antibody (Abcam), and goat anti–β-catenin antibody (Novus).

Quantitative RT-PCR. Total RNA was isolated from renal tissues and reverse transcribed to cDNA. Oligonucleotides were designed using Primer3 software (bioinfo.ut.ee/primer3-0.4.0/). Primers of AQP2 were 5′-gctgtcaatgctctccacaa-3′ (sense) and 5′-ggagcaaccggtgaaataga-3′ (antisense); primers for GAPDH were 5′-gtcttcactaccatggagaagg-3′ (sense) and 5′-tcatggatgaccttggccag-3′ (antisense).

Cell Membrane and Cytoplasmic Protein Fraction Isolation. The membrane and cytosolic fractions of proteins were extracted using a kit according to the manufacturer's instructions (catalog no. BSP002; Bio Basic Inc.).

Coimmunoprecipitation. For coimmunoprecipitation with PRR and FZD8, the membrane fraction of rat renal inner medullary was performed using a kit (catalog no. BSP002; Bio Basic Inc.). Anti–PRR-N (from Y.F.) or anti-FZD8 (Santa Cruz) antibody was cross-linked with the magnetic beads (catalog no. 88805; Pierce) and then incubated for 30 min with the renal medullary membrane proteins. The beads were collected, washed, and eluted. The immunoprecipitated samples were analyzed for the binding partner by immunoblotting.

siRNA or Plasmid Transfection in Primary Cultured IMCD Cells. IMCD cells were transfected with FZD8 siRNA oligonucleotides (Invitrogen) or the luciferase reporter plasmid (catalog no. CCS-018L; Qiagen) at a final concentration of 5 nM using HiPerFect transfection reagent (catalog no. 301702; Qiagen) for 72 h. The efficiency of FZD8 knockdown was validated by immunoblotting of FZD8. For the luciferase assay, each sample consisted of a positive control, a negative control, and a target luciferase construct, and the reporter activity was calculated according to the manufacturer's instruction.

Preparation of Luciferase Constructs. Genomic DNA was extracted from rat tail using a Tissue DNA kit (D3396-01; Promega). A 2,016-bp fragment of the 5′ flanking region of the PRR gene (GenBank accession no. NM_001007091; 1,941 ± 75 bp) was amplified from the rat genomic DNA by PCR and subcloned to the pGL3-Basic reporter vector (Promega) using NheI and BglII restriction sites; this construct was termed "pGL3-PRR." A 2,084-bp fragment of the 5′ flanking region of the AQP2 gene (GenBank accession no. NM_012909; 2,000 ± 84 bp) was cloned to the pGL3-Basic reporter vector by a similar strategy; this construct was termed "pGL3-AQP2." The identity of these constructs was validated by sequencing.

Luciferase Assay. The mpkCCD cells were transfected with pGL3-AQP2 plasmid or empty vector by using HiPerFect Transfection Reagent (catalog no. 301702; Qiagen). Upon confluence, all cells were starved for 12 h; then pGL3-PRR- and pGL3AQP2-transfected cells were treated for 24 h with TO901317 (10 μM) or sPRR-His (10 nM), respectively. The vehicle-treated group served as a control. The luciferase activities were measured using a luciferase assay system (Promega), and luminescence was detected by using an illuminometer (BMG FLUOstar OPTIMA).

Statistical Analysis. Data are summarized as means ± SE. Statistical analysis was performed using ANOVA with the Bonferroni test for multiple comparisons or paired or unpaired Student's *t* test for two comparisons. $P < 0.05$ was considered statistically significant.

ACKNOWLEDGMENTS. We thank Dr. John Lewicki (OncoMed Pharmaceuticals) for providing the FZD8 inhibitor OMP-54F03. This work was supported by National Natural Science Foundation of China Grants 91439205 and 31330037; NIH Grants DK094956 and DK104072; National Basic Research Program of China 973 Program 2012CB517600 Grant 2012CB517602; and by the Veterans Administration Merit Review. T.Y. is a Research Career Scientist in the Department of Veterans Affairs. J.-Å.G. was supported by the Swedish Science Council and by Grant E-0004 from the Robert A. Welch Foundation. Y.F. was supported by Grant NHLBI/R01HL122770 from the NIH.

1. Nguyen G (2011) Renin and prorenin receptor in hypertension: What's new? *Curr Hypertens Rep* 13(1):79–85.
2. Watanabe N, et al. (2012) Soluble (pro)renin receptor and blood pressure during pregnancy: A prospective cohort study. *Hypertension* 60(5):1250–1256.
3. Nguyen G, et al. (2002) Pivotal role of the renin/prorenin receptor in angiotensin II production and cellular responses to renin. *J Clin Invest* 109(11):1417–1427.
4. Kinouchi K, et al. (2010) The (pro)renin receptor/ATP6AP2 is essential for vacuolar H+-ATPase assembly in murine cardiomyocytes. *Circ Res* 107(1):30–34.
5. Cousin C, et al. (2009) Soluble form of the (pro)renin receptor generated by intracellular cleavage by furin is secreted in plasma. *Hypertension* 53(6):1077–1082.
6. Yoshikawa A, et al. (2011) The (pro)renin receptor is cleaved by ADAM19 in the Golgi leading to its secretion into extracellular space. *Hypertens Res* 34(5): 599–605.
7. Maruyama N, Segawa T, Kinoshita N, Ichihara A (2013) Novel sandwich ELISA for detecting the human soluble (pro)renin receptor. *Front Biosci (Elite Ed)* 5: 583–590.
8. Fukushima A, et al. (2013) Increased plasma soluble (pro)renin receptor levels are correlated with renal dysfunction in patients with heart failure. *Int J Cardiol* 168(4): 4313–4314.
9. Hamada K, et al. (2013) Serum level of soluble (pro)renin receptor is modulated in chronic kidney disease. *Clin Exp Nephrol* 17(6):848–856.
10. Watanabe N, et al. (2013) Prediction of gestational diabetes mellitus by soluble (pro)renin receptor during the first trimester. *J Clin Endocrinol Metab* 98(6):2528–2535.
11. Morimoto S, et al. (2014) Serum soluble (pro)renin receptor levels in patients with essential hypertension. *Hypertens Res* 37(7):642–648.
12. Nguyen G, et al. (2014) Plasma soluble (pro)renin receptor is independent of plasma renin, prorenin, and aldosterone concentrations but is affected by ethnicity. *Hypertension* 63(2):297–302.
13. Advani A, et al. (2009) The (Pro)renin receptor: Site-specific and functional linkage to the vacuolar H+-ATPase in the kidney. *Hypertension* 54(2):261–269.
14. Wang FLX, et al. (2016) Antidiuretic action of collecting duct (pro)renin receptor downstream of vasopressin/EP4 receptor. *J Am Soc Nephrol*, in press.

15. Ramkumar N, et al. (2015) Nephron-specific deletion of the prorenin receptor causes a urine concentration defect. *Am J Physiol Renal Physiol* 309(1):F48–F56.
16. Berkenstam A, Gustafsson JA (2005) Nuclear receptors and their relevance to diseases related to lipid metabolism. *Curr Opin Pharmacol* 5(2):171–176.
17. Alberti S, Steffensen KR, Gustafsson JA (2000) Structural characterisation of the mouse nuclear oxysterol receptor genes LXRalpha and LXRbeta. *Gene* 243(1-2): 93–103.
18. Zelcer N, Hong C, Boyadjian R, Tontonoz P (2009) LXR regulates cholesterol uptake through Idol-dependent ubiquitination of the LDL receptor. *Science* 325(5936): 100–104.
19. Repa JJ, Mangelsdorf DJ (2000) The role of orphan nuclear receptors in the regulation of cholesterol homeostasis. *Annu Rev Cell Dev Biol* 16:459–481.
20. Repa JJ, et al. (2000) Regulation of absorption and ABC1-mediated efflux of cholesterol by RXR heterodimers. *Science* 289(5484):1524–1529.
21. Caldas YA, et al. (2011) Liver X receptor-activating ligands modulate renal and intestinal sodium-phosphate transporters. *Kidney Int* 80(5):535–544.
22. Kittayaruksakul S, Soodvilai S, Asavapanumas N, Muanprasat C, Chatsudthipong V (2012) Liver X receptor activation downregulates organic anion transporter 1 (OAT1) in the renal proximal tubule. *Am J Physiol Renal Physiol* 302(5):F552–F560.
23. Soodvilai S, Jia Z, Fongsupa S, Chatsudthipong V, Yang T (2012) Liver X receptor agonists decrease ENaC-mediated sodium transport in collecting duct cells. *Am J Physiol Renal Physiol* 303(12):F1610–F1616.
24. Li W, et al. (2012) Brain-targeted (pro)renin receptor knockdown attenuates angiotensin II-dependent hypertension. *Hypertension* 59(6):1188–1194.
25. Gonzalez AA, Luffman C, Bourgeois CR, Vio CP, Prieto MC (2013) Angiotensin II-independent upregulation of cyclooxygenase-2 by activation of the (Pro)renin receptor in rat renal inner medullary cells. *Hypertension* 61(2):443–449.
26. Huang SM, et al. (2009) Tankyrase inhibition stabilizes axin and antagonizes Wnt signalling. *Nature* 461(7264):614–620.
27. Smith S, Giriat I, Schmitt A, de Lange T (1998) Tankyrase, a poly(ADP-ribose) polymerase at human telomeres. *Science* 282(5393):1484–1487.
28. Nielsen S, et al. (2002) Aquaporins in the kidney: From molecules to medicine. *Physiol Rev* 82(1):205–244.
29. Knepper MA, et al. (1996) Renal aquaporins. *Kidney Int* 49(6):1712–1717.
30. Fujiwara TM, Bichet DG (2005) Molecular biology of hereditary diabetes insipidus. *J Am Soc Nephrol* 16(10):2836–2846.
31. Wesche D, Deen PM, Knoers NV (2012) Congenital nephrogenic diabetes insipidus: The current state of affairs. *Pediatr Nephrol* 27(12):2183–2204.
32. Morello F, et al. (2005) Liver X receptors alpha and beta regulate renin expression in vivo. *J Clin Invest* 115(7):1913–1922.
33. Gabbi C, et al. (2012) Central diabetes insipidus associated with impaired renal aquaporin-1 expression in mice lacking liver X receptor β. *Proc Natl Acad Sci USA* 109(8):3030–3034.
34. Tachibana H, et al. (2012) Activation of liver X receptor inhibits osteopontin and ameliorates diabetic nephropathy. *J Am Soc Nephrol* 23(11):1835–1846.
35. Wang F, et al. (2014) Prostaglandin E-prostanoid4 receptor mediates angiotensin II-induced (pro)renin receptor expression in the rat renal medulla. *Hypertension* 64(2): 369–377.
36. Jung HJ, et al. (2015) Tankyrase-mediated β-catenin activity regulates vasopressin-induced AQP2 expression in kidney collecting duct mpkCCDc14 cells. *Am J Physiol Renal Physiol* 308(5):F473–F486.
37. Cruciat CM, et al. (2010) Requirement of prorenin receptor and vacuolar H+-ATPase-mediated acidification for Wnt signaling. *Science* 327(5964):459–463.
38. Oshima Y, Morimoto S, Ichihara A (2014) Roles of the (pro)renin receptor in the kidney. *World J Nephrol* 3(4):302–307.
39. Rousselle A, Sihn G, Rotteveel M, Bader M (2014) (Pro)renin receptor and V-ATPase: From Drosophila to humans. *Clin Sci (Lond)* 126(8):529–536.
40. Krop M, Lu X, Danser AH, Meima ME (2013) The (pro)renin receptor. A decade of research: What have we learned? *Pflugers Arch* 465(1):87–97.
41. Song R, Preston G, Ichihara A, Yosypiv IV (2013) Deletion of the prorenin receptor from the ureteric bud causes renal hypodysplasia. *PLoS One* 8(5):e63835.
42. Yasui M, Zelenin SM, Celsi G, Aperia A (1997) Adenylate cyclase-coupled vasopressin receptor activates AQP2 promoter via a dual effect on CRE and AP1 elements. *Am J Physiol* 272(4 Pt 2):F443–F450.
43. Zharkikh L, et al. (2002) Renal principal cell-specific expression of green fluorescent protein in transgenic mice. *Am J Physiol Renal Physiol* 283(6):F1351–F1364.
44. Lu X, et al. (2015) Activation of ENaC in collecting duct cells by prorenin and its receptor PRR: Involvement of Nox4-derived hydrogen peroxide. *Am J Physiol Renal Physiol*, 10.1152/ajprenal.00492.2015.
45. Kim RJ, Malattia C, Allen M, Moshang T, Jr, Maghnie M (2004) Vasopressin and desmopressin in central diabetes insipidus: adverse effects and clinical considerations. *Pediatr Endocrinol Rev* 2(Suppl 1):115–123.
46. Granger JP, West D, Scott J (1994) Abnormal pressure natriuresis in the dog model of obesity-induced hypertension. *Hypertension* 23(1, Suppl):I8–I11.
47. West DB, Wehberg KE, Kieswetter K, Granger JP (1992) Blunted natriuretic response to an acute sodium load in obese hypertensive dogs. *Hypertension* 19(1, Suppl): I96–I100.
48. Spark RF, Arky RA, Boulter PR, Saudek CD, O'Brian JT (1975) Renin, aldosterone and glucagon in the natriuresis of fasting. *N Engl J Med* 292(25):1335–1340.
49. Weinsier RL (1971) Fasting–a review with emphasis on the electrolytes. *Am J Med* 50(2):233–240.
50. Zhang H, et al. (2005) Collecting duct-specific deletion of peroxisome proliferator-activated receptor gamma blocks thiazolidinedione-induced fluid retention. *Proc Natl Acad Sci USA* 102(26):9406–9411.
51. Guan Y, et al. (2005) Thiazolidinediones expand body fluid volume through PPARgamma stimulation of ENaC-mediated renal salt absorption. *Nat Med* 11(8):861–866.
52. Kuipers I, et al. (2010) Activation of liver X receptor-alpha reduces activation of the renal and cardiac renin-angiotensin-aldosterone system. *Laboratory Investigation* 90(4):630–636.
53. Wang F, et al. (2015) Renal medullary (pro)renin receptor contributes to angiotensin II-induced hypertension in rats via activation of the local renin-angiotensin system. *BMC Med* 13:278.